THE MÖSSBAUER EFFECT

INTRODUCTION

In this experiment you will observe the Mössbauer effect (the recoil-free emission and absorption of gamma rays from nuclear transitions) and use Mössbauer spectroscopy to examine the properties of recoil-free radiation processes and investigate the effects of environmental factors on the energy levels of the nucleus.

In quantum mechanics, the nucleus can be treated in much the same way as the atom. Although the details of nuclear binding differ considerably from the Coulomb binding of the atom, both the atom and the nucleus are multiparticle systems subject to the same sort of quantum mechanical analysis. In particular, just like the atom, the nucleus has quantized energy levels. Although the nucleus generally occupies the ground state energy level, it can be excited to higher levels and make transitions back to lower levels, absorbing or emitting photons in the process. While atomic (electronic) transitions have energies in the eV to keV range, nuclear gamma rays have energies on the order of keV to MeV. Reminder: photons that originate from atomic deexcitations are called x-rays, and those from nuclear deexcitations are γ-rays.

Transitions between nuclear states generally occur by radiation processes involving recoil. In recoil emission, conservation of momentum requires the nucleus to carry away momentum equal and opposite to that of the emitted gamma ray. The kinetic energy of the nucleus necessarily takes up some of the energy available from the transition. As a result, there is less energy left for the gamma, and its energy is lower than the energy released by the transition. Conversely, absorption with recoil requires a gamma ray of energy greater than the energy of the transition, as some of the energy is again taken up by the kinetic energy of the nucleus. The energy shifts of the gammas in emission and absorption are large compared to the width of the transition line (determined by the lifetime of the state according to the Heisenberg relation, $\Delta E \Delta t \geq \hbar$). You should calculate the value of the energy shift for some typical example(s). Because the overlap is minimal, a gamma emitted by a nucleus in a transition from state 2 to state 1 generally cannot excite the transition from state 1 to state 2 in another nucleus of the same element.

In 1957 Rudolf Mössbauer, a graduate student at the Max-Planck Institut in Heidelberg, discovered the recoil-free emission and absorption of gamma rays from nuclear transitions, a discovery for which he was awarded the Nobel Prize three years later at the age of thirty-two. The essence of the Mössbauer effect is the absorption of recoil momentum by the entire lattice of the solid. Since the lattice is much more massive than the nucleus, its recoil kinetic energy is effectively zero. In this case the gamma ray carries away exactly the energy of the transition, and the emission and absorption lines overlap, centered about the transition energy. Suppose a nucleus emits a gamma ray (without recoil) of energy E_γ in making the transition from state 2 to state 1. The overlap between emission and absorption lines allows another nucleus to absorb that gamma ray in going from state 1 to state 2. Such resonant absorption is the key to Mössbauer spectroscopy. The probability of recoil free emission/absorption can be calculated using quantum mechanics.

Given the possibility of recoil-free emission and absorption, one can use resonant absorption to examine energy profiles of nuclear transitions. The range of energies incident on an absorber can be precisely shifted by one part in 10^{13} or so (energies on the order of μeV or neV) using the Doppler effect: radiation emitted by a source moving with velocity v has an energy shift $\Delta E = (v/c)E_\gamma$, where E_γ is the unshifted gamma-ray energy.[1] By varying the velocity, and thus the energy shift, it is possible to scan through a range of energies on the order of those for natural line widths of nuclear processes, for temperature shifts in the nuclear transition lines, and for hyperfine structure in the energy levels. The shifted gamma rays are absorbed in proportion to the overlap of the shifted emission line with the absorption line. Thus the relative absorption at different energy shifts reveals much information about the details of the nuclear energy levels. Even more importantly, for solid-state physics, it serves to test lattice vibrational models predicting the fraction of recoil-free processes, as well as to provide data on the environment of the nucleus in the lattice -- e.g., internal magnetic fields, Coulomb interactions with atomic electrons, and quadrupole interactions with field gradients, among many other effects. The (1) depth of the absorption line(s), (2) width, (3) energy and, (4) the number of lines observed provide the experimental information. This is summarized in Table 1.2 (Mössbauer parameter and effects) reproduced from Gonser [1975]. An outline of some of the theory follows, but the references and original papers need to be consulted for explanations and derivations.

[1]To gain an appreciation for the minuteness of this Doppler shift, R.V. Pound has given the following analogy. Imagine a tuning fork attached to the end of the hour hand of a clock. The acoustic Doppler shift due to the motion of the tuning fork on the hour hand is many orders of magnitude greater than the shifts encountered in the Mössbauer effect.

Table 1.2. Mössbauer parameters and effects U. Gonser, Mössbauer Spectroscopy pp 16-17.

Symbol	Definition and units used	Corresponds in wave or particle picture, respectively	Physical parameter	Cause of the effects	Observed or predicted effects	Formulation	Fe^{57} energy level diagram with allowed transitions (Source (S) / Absorber (A))	Schematic representation of observation (resonance absorption vs. velocity)
f	Number of recoil free γ-ray events (emission or absorption) divided by total number of γ-ray events, dimensionless (Debye-Waller factor)	Relative intensity of resonance line Probability of recoil-free events	Probability of phonon creation or annihilation by the emitting or absorbing atom or mean square of vibrational amplitude		Intensity of Mössbauer line	$f = \exp - k^2 \langle x^2 \rangle$	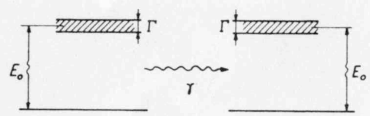	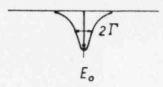
				Vibrational modes of the resonating atom (as function of direction, temperature and pressure, in different lattices, phases, near critical temperatures, at surfaces and close to other lattice defects)	Intensity dependence			
				Vibrational modes of the resonating atom in non-cubic symmetry of single crystals, and polycrystalline materials	Change in the relative line intensities of hyperfine split spectra (Goldanskii-Karyagin effect)			
Γ	Full width at half maximum in energy units	Line width or spread in wave length Uncertainty or spread in energy	Mean lifetime of the excited state Apparent mean lifetime of the excited state Atomic, magnetic electric relaxation processes	Saturation effects Diffusion and Brownian motion of the atoms or molecules, Relaxation processes, Spin-flip processes, Superparamagnetism, Fluctuations near critical temperatures (magnetic, ferroelectric and other phase transitions) Delay coincidence measurements Thermal spike Change in the mean lifetime of the excited state	Natural line width } Line broadening } Line narrowing Line narrowing or line broadening	$\Gamma_{eff} = \frac{\hbar}{\tau_{eff}}$	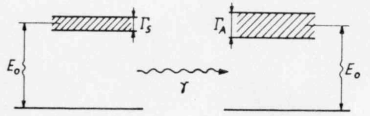	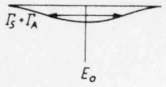
E_γ	Mean energy of radiation in energy units	Mean wavelength of γ-radiation Mean energy of γ-radiation	Energy difference between excited and ground state	Interaction of the nuclear charge distribution with the electron density at the nuclei in source and absorber (electric monopole interaction)	Isomer shift	$\delta = C \frac{\delta R}{R} [\lvert\psi_A(0)\rvert^2 - \lvert\psi_S(0)\rvert^2]$	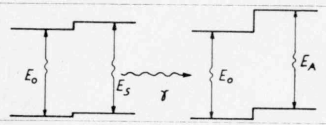	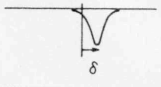
				Interaction of the nuclear magnetic dipole moment with a magnetic field at the nucleus (magnetic dipole interaction); Angular dependence of the nuclear Zeeman effect in single crystals, preferred oriented materials (texture) and polycrystalline materials; Symmetry tests in γ-decay (time reversal invariance, parity conservation); Boltzmann population of the hyperfine sublevels at low temperature ($\ll 1$ K)	Nuclear Zeeman effect Change in the relative line intensities, polarization of the γ-radiation (linear, elliptical, circular) Change in relative line intensities Change in relative line intensities	$E_m = -g_N \beta_N H m_I$	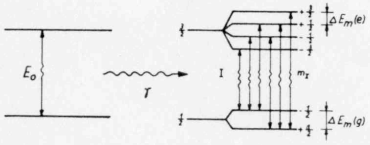	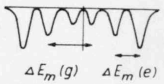
				Interaction of the nuclear quadrupole moment with EFG at the nucleus (electric quadrupole interaction) Angular dependence of the quadrupole interaction in single crystals, preferentially oriented materials (texture) and polycrystalline materials	Quadrupole splitting Change in the relative line intensities, polarization of the γ-radiation	$E_Q = \pm \frac{1}{4} eQV_{zz} (1 + \frac{1}{3}\eta^2)^{\frac{1}{2}}$	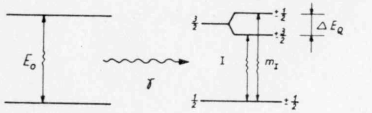	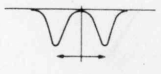
				Change in temperature Change in pressure Acceleration and gravitational fields	Temperature shift Pressure shift Acceleration and gravitational red shift	$\delta_R = \frac{v^2}{2c^2} E_\gamma$	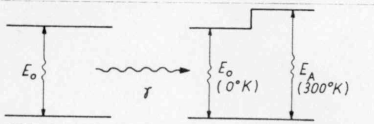	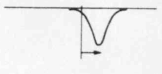

Hyperfine interaction

Relativistic effects

THEORY

We begin by considering what determines the depth and width of the Mössbauer absorption line. This is followed by brief discussions of the various phenomena affecting the absorption line(s). The (1) isomer shift, (2) nuclear Zeeman effect, and (3) quadrupole splitting are due to hyperfine interactions, while the (4) temperature shift is a relativistic effect.

(a) ***Recoil-free fraction:*** The depth of the Mössbauer resonance is determined by the fraction of recoil-free emissions in the source and the resonant absorption cross section in the absorber (as well as photoelectric and Compton scattering). The recoil-free fraction of the source is defined to be the fraction of gamma rays that is emitted without recoil. Similarly, the recoil-free fraction of the absorber is the fraction that is absorbed without recoil. Since recoil-free processes occur when the recoil momentum is taken up by the entire lattice, the fraction depends on the structure of the lattice. Solid-state physics tells us that lattice vibrations are quantized, coming only in packets called phonons. Particular theories provide different spectra of lattice vibrations. Accordingly, the recoil-free fraction depends of the phonon spectrum that a given theory predicts. The expression for the recoil-free fraction in the Debye theory is called the Debye-Waller factor, f:

$$f = \exp\left(-\frac{E_\gamma^2}{(\hbar c)^2} \langle x \rangle^2 \right)$$

where E_γ is the gamma energy, and $\langle x \rangle^2$ is the mean square displacement of the atom in its thermal vibrations about its origin (see Frauenfelder, for example); f will only be large for small values of gamma energy and for tightly bound atoms. The Debye theory of lattice vibrations gives an estimate for the mean square displacement of the atom and thus f can be evaluated. However, the finite thickness of the absorber modifies the recoil-free fraction. On one hand, a thin absorber cannot absorb all the recoil-free gamma rays because there are not enough nuclei in their path to ensure an interaction. On the other hand, a thick absorber offers more chances for an incident gamma ray to be absorbed with recoil. The thickness of the absorber thus changes the observed absorption so that it no longer equals the recoil-free fraction of the source. Corrections for the thickness can be applied to the measured absorption and then compared to the recoil-free fraction, which is predicted by the Debye theory. If the values are consistent, one can consider the Debye theory an adequate description of the lattice for this purpose.

(b) ***Natural linewidth:*** Assuming the nuclei in the source are decaying exponentially, the energy distribution of the emitted gamma rays can be shown to be Lorentzian:

$$N(E) = \frac{N_o}{(E - E_\gamma)^2 + (\Gamma / 2)^2}.$$

Here E_γ is the central energy of the distribution and $\Gamma = \hbar/\tau$ is the full width at half-maximum (FWHM) of the emission line (see Greenwood & Gibb). The absorption line has the same Lorentzian shape with the same linewidth Γ. The shapes of the emission and absorption lines determine the observed absorption curve. In particular, it is Lorentzian with an observed linewidth of Γ_{obs}. If the source is infinitely thin, all the recoil-free emitted gamma rays escape from the source, and no unwanted interactions broaden the emission line. Similarly, if the absorber is infinitely thin, the least number of incident gamma rays are lost to non-resonant absorption. In this ideal case, the observed linewidth is simply the sum of the emission and absorption linewidths, giving $\Gamma_{obs} = \Gamma + \Gamma = 2\,\Gamma$. However, the ideal case is impractical for reasons of signal-to-noise ratio. In more realistic situations in which both the source and absorber thickness is finite, it no longer holds that $\Gamma_{obs}/\ \Gamma = 2$. Instead, non-resonant processes broaden the observed absorption curve, and corrections have been developed by workers in Mössbauer spectroscopy. Using these correction formulas one can calculate the linewidth Γ of the absorption and emission processes from the observed FWHM Γ_{obs} of the absorption curve. By the Heisenberg principle, the linewidth of the radiation and the lifetime of the excited state are related by $\Delta E \Delta t \geq \Gamma/\tau = \hbar$. The linewidth thus allows one to calculate the lifetime of the state for comparison with the accepted value, 1.4×10^{-7} sec.

(c) ***Isomer shift (chemical shift):*** In many cases it is sufficient to treat the Coulomb interaction between the atomic electrons and the nucleus as though the nucleus were a point charge. With this assumption, the electronic wavefunctions would not overlap at all with the nucleus. However, this is not the case and the s-electrons in particular have a finite probability of being found within the nuclear volume. The overlap between the electrons and the nucleus produces a change in energy due to Coulomb interaction, which in turn changes the total energy of the system.

Suppose that the ground and excited states of the nucleus have slightly different radii. Then the overlap between nucleus and electrons will be different for the two states. Consequently, the change in energy will also be different. This difference shows up as a shift of the peak away from the resonance energy E_γ. The isomer shift appears in some degree in all samples

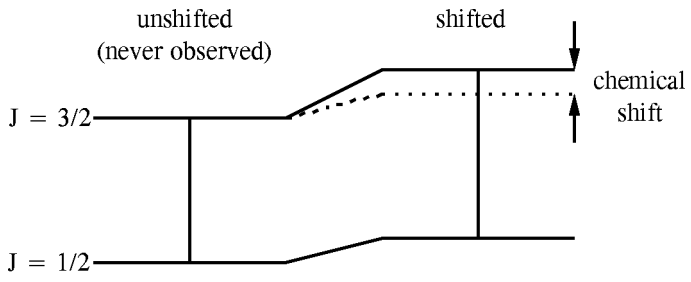

origin of the chemical shift

because the electrons always overlap to some extent with the nucleus. Thus Mössbauer spectra are never exactly centered about zero energy shift, or zero velocity.

(d) ***Zeeman effect (magnetic hyperfine splitting):*** A nucleus can have a characteristic angular momentum, J, which is accompanied by a magnetic dipole moment. When the nucleus is placed in a magnetic field, the energy states are split, with energies depending on the orientation of the nuclear moment with respect to the field. A state with quantum number J can split into 2J+1 components characterized by the quantum number m_J. The splitting of the energy levels is called the nuclear Zeeman effect and is exactly analogous to the Zeeman effect of atomic physics.

The splitting of the energy states produces a splitting of the line corresponding to the transition between two states. In Fe-57, we are looking at the transition between the J=1/2 and J=3/2 levels. The presence of a magnetic field splits the levels as shown.

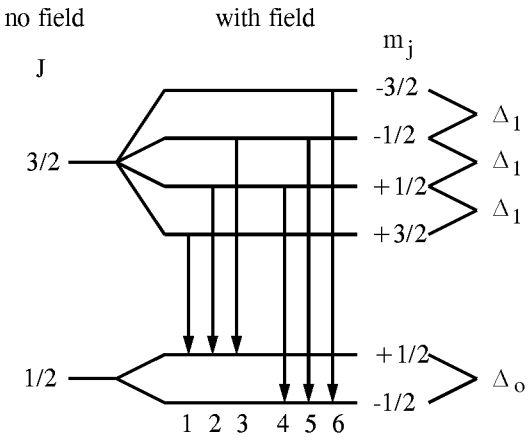

allowed transitions between Zeeman split J=3/2 and J=1/2 levels

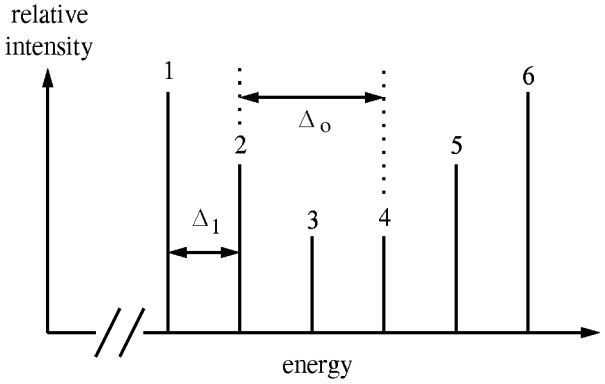

relative energies and intensities for allowed transitions

There are nominally eight possible transitions. Since these are magnetic dipole transitions, the selection rule $\Delta m_J = -1, 0, +1$ becomes operative. That rules out two transitions, leaving six lines that are observed. The separations between the levels are given just as in the Zeeman effect:

$$\Delta_o = g_o \mu_N H = \mu_o H / J_o$$
$$\Delta_1 = g_1 \mu_N H = \mu_1 H / J_1$$

where μ_N is the nuclear magneton and g_o and g_1 are called the g-factors for the J=1/2 and J=3/2 levels. If we measure the energy splittings and know the g-factors, we can calculate the strength of the magnetic field at the nucleus, a quantity of interest in solid-state physics.

If we assume that the magnetization is randomly directed, the intensities of the lines, given by a detailed quantum mechanical calculation, come in the ratio 3:2:1:1:2:3. Random magnetization can sometimes be obtained with thin foils of iron, which are often slightly magnetized. On the other hand, if a uniformly directed magnetic field is applied, the intensity ratio is 3:x:1:1:x:3, where $x = 4 \sin^2\theta / (1+ \cos^2 \theta)$. Here θ is the angle between the direction of magnetization and the direction of radiation. When observing magnetic hyperfine splitting, it is best to have only one of the source or absorber be magnetic. Otherwise there would be six emission and six absorption lines and the spectrum would be quite complex. Since we cannot change the source, we use an absorber of metallic Fe, preferably enriched in Fe-57.

(e) ***Quadrupole splitting:*** The nucleus is held in position in its environment by Coulomb forces. The fact that it is stationary (neglecting thermal vibrations) implies that there can be no electric field at the nucleus; if there were, the nucleus would move to a point of no field. However, there can be a gradient in the electric field. A field gradient could arise, for example, from a non-spherically symmetric distribution of atoms in the lattice, as shown in the figure. [Calculate the field gradients at the center of a square (the site of the Fe atom in the figure) with charges +q at the corners, distance a from the center.]

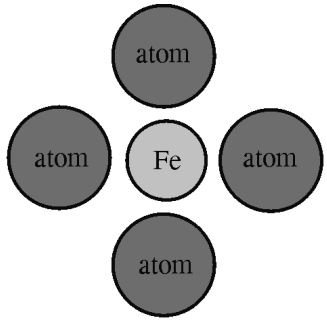

possible condition for quadrupole splitting

If a nucleus in a particular spin state has a slight spheroidal deformation, its distribution of charge is not perfectly spherical, and the nuclear quadrupole moment, Q, is a measure of the deviation of the nuclear charge from spherical symmetry. If a nucleus has a quadrupole moment, its energy depends on its orientation with respect to the electric field gradient. The energy of a level with quantum numbers J and m_J is shifted from its zero-gradient level by

$$\Delta E = e^2 qQ \frac{3m_J^2 - J(J+1)}{4J(2J-1)}$$

if the field gradient is axially symmetric, where $q = \frac{1}{e}\frac{dE}{dz}$ measures the field gradient. Note that the quadrupole splitting, unlike the magnetic splitting, does not depend on the sign of m_J but only on its magnitude. This happens because the spheroidally deformed nucleus, unlike a spin or magnetic moment, has no preference between up and down.

In Fe-57, the J=3/2 state is split into two components. Application of the formula shows the two levels are symmetric about the unsplit energy. The J=1/2 level, however, is spherically symmetric and shows no splitting. With an absorber containing Fe-57 in a suitable material, one sees two lines of equal intensity, equally spaced about the resonance energy.

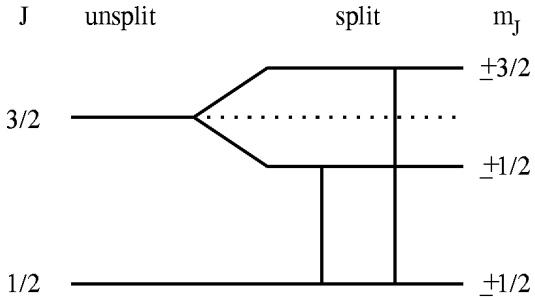

quadrupole splitting of energy levels

If we measure the energy difference between the two lines in the spectrum, we can use the formula for the energy shift to find Q dE/dz, the product of the quadrupole moment for J=3/2 and the electric field gradient. If we further know the quadrupole moment from nuclear experiments, we can estimate the field gradient at the nucleus.

(f) ***Temperature shift (2nd-order Doppler shift):*** The thermal vibrations of nuclei can shift the frequency of their recoil free radiation by means of the relativistic Doppler effect. One can understand this shift by remembering that moving clocks, according to special relativity, run slow. Since the nucleus is moving, an observer in the lab frame perceives a nuclear-frame clock to run slow. For instance, suppose a lab-frame observer finds that 1 second passes in the lab frame while the nuclear-frame clock ticks off 0.5 sec. If the nucleus radiates with a frequency ν_o = 2 Hz in accordance with its own clock, it would emit one wavelength in 0.5 sec as read on its clock. However, during this time the observer sees 1 sec pass on the lab-frame clock, yet only one wavelength has emerged. The lab-frame observer will say that the frequency is not 2 Hz but 1 Hz: the observed frequency has been shifted downwards by the factor by which moving clocks run slow, namely $\sqrt{1-(v/c)^2}$. Since $\langle v \rangle^2$ increases with temperature, the energy of the gamma ray shifts lower as the temperature is increased.

(g) Antiferromagnetic transition in ferrous fluoride: If the iron atom is in a lattice that undergoes a transition to ferromagnetic or antiferromagnetic (AF) order, then the lattice of iron atoms is magnetized. We focus on the AF case. The iron nuclear spin will interact with the sublattice magnetization M via the hyperfine interaction; hyperfine effective magnetic fields can

be enormous, splitting the ground and excited states, enabling the internal hyperfine field to be determined. In the paramagnetic state the average of the magnetization is zero, whereas the ordering breaks the symmetry and the sublattice magnetization or the hyperfine field is non-zero as in the figure below for the antiferromagnet, FeF_2.

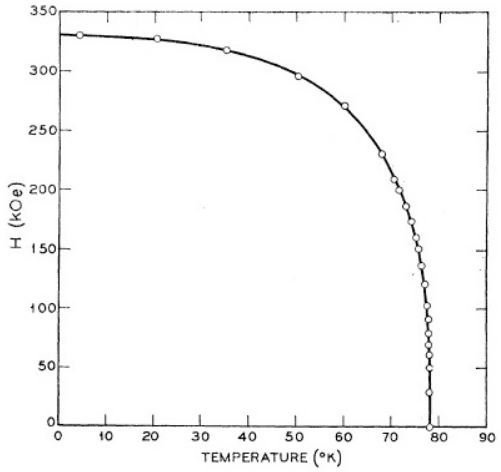

The hyperfine effective field as a function of temperature in FeF_2.

The sublattice magnetization M is the order parameter for an antiferromagnet; thus the Mössbauer effect can be used to determine the order parameter. Above the Néel temperature T_N the M is zero whereas below it rises as a power law

$$M(T) = M_0(1 - T / T_N)^{\beta},$$

valid in the vicinity of the transition. The exponent β is called the critical exponent and extensive theory shows that it has a value of around 1/3.

APPARATUS

In this section we give a general description of the various components. Detailed information, especially *instruction manuals* and *spec sheets* can be found with the *Bench Notes*. Be sure to read these, but they are to remain in the lab, i.e. *do not take them home to read.* Copies of the Bench Notes are available on the course web site.

- Co^{57} source (in palladium matrix) mounted on velocity driver (loudspeaker)
- velocity transducer (Sanborn LVsyn 6LV2)
- driver control unit (laboratory-built)
- proportional counter (Reuter-Stokes RSG-61) with H.V. power supply (Ortec 478)
- proportional counter preamp (Canberra 806)

- spectroscopy amplifier (Ortec 570)
- single channel analyzer (Ortec 551)
- linear gate and pulse stretcher (Ortec 542)
- multichannel analyzer (computer-based)
- oscilloscope (Tektronix 2225)
- universal counter (Hewlett Packard 5315A)
- liquid nitrogen cryostat (Precision Cryogenic Systems PCS 4-06-102) with cold finger
- mechanical vacuum pump
- temperature controller (Lake Shore 330)
- Michelson interferometer for velocity calibration (5mW HeNe laser, beam splitter, mirrors and photodetector)
- various absorbers, including Fe enriched in Fe^{57}, Fe_2O_3 (ferric oxide), $K_4Fe(CN)_6 \cdot 3H_2O$ (potassium ferrocyanide), $Na_4Fe(CN)_6 \cdot 10H_2O$ (sodium ferrocyanide), FeF_2 (ferrous fluoride), FeS_2, FeS (ferrous sulfide), stainless steel (the stainless steel absorbers are available in thicknesses from 0.2 to 3 mils), garnet, permalloy, and others.

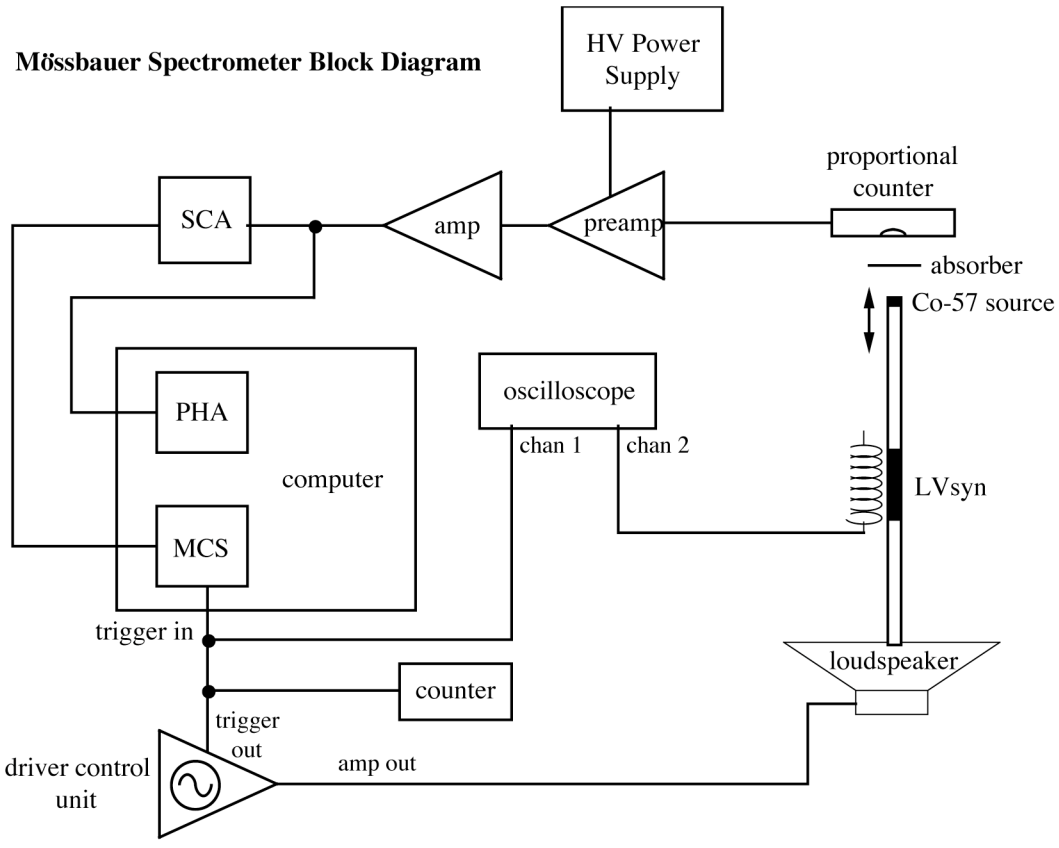

Radiation source: Co^{57} (half-life = 270 days) decays by K-electron capture to Fe^{57} in the nuclear excited state with J=5/2 to J=3/2. The 14.41 keV line is emitted when the J=3/2 excited state in Fe^{57} decays to the J=1/2 ground state with a lifetime of $\tau = 1.4 \times 10^{-7}$ sec. The Co^{57} has been electrodeposited on a Palladium matrix and has an active diameter of 6 mm; the foil is held in a "Ranger" type mount, which, in turn is attached to the *velocity transducer*. A lead shield surrounds it. The source strength was 5.0 mCi on 1 September 2006. Although the source has been sprayed with an acrylic coating it is NOT a sealed source and, if necessary, should be HANDLED WITH CARE. Make sure you review and follow the *radiation safety procedures* outlined on pages 6-8 of the Introduction in this Laboratory Manual.

Velocity driver/transducer: To produce the variable overlap between emission and absorption lines, the emission line from the Fe^{57} is Doppler shifted by moving the Co^{57} source. The source is connected to a loudspeaker, which is driven harmonically by a sinusoidal voltage supplied by the *driver control unit*. The connecting rod between the Co^{57} source and the loudspeaker is a *velocity transducer*. It consists of two parts: a shielded cylindrical coil assembly and a permanent magnet. The relative motion of the magnet and the coil generates a voltage whose magnitude is proportional to the velocity, and whose polarity indicates the direction of motion. The sensitivity is about 225 mV cm^{-1} sec (open circuit), but this is something you should calibrate as described in the *Experimental Procedure* section. The output signal from the LVsyn velocity transducer is available at the blue Pomona box mounted on the tripod support over the speaker, and can be monitored on the scope. (The BNC jack and the coax cable coming out of the box are wired in parallel.) Note that the *position* and *velocity* of the source are 90˚ out of phase with each other.

Detector: The detector is a proportional counter featuring a 1" diameter, 0.010" thick (46 mg/cm^2), beryllium side window -- USE EXTREME CAUTION NOT TO PUNCTURE THE WINDOW. The counter is filled with a mixture of Xe-CO_2 gas at one atmosphere pressure. The (instrumental) line width for the 14 keV line is 1.3 keV, giving it about a 10% (FWHM) resolution at that energy. Its efficiency is 67% at 14.4 keV (and 89% at 6.5 keV). The bias voltage (+1850 V) is supplied by a H.V. power supply located in the NIM Bin Crate. It is fed through the preamp to the counter; the cable (with MHV connectors) that connects the preamp to the counter also carries the signal.

Driver control unit: The driver control unit is a precision oscillator/amplifier located in the NIM Bin Crate. It provides the 10-100 Hz sinusoidal driving voltage for the loudspeaker. (The universal counter is used to accurately determine and monitor the period of this sine wave; use

the *period* mode of operation.) The controls on the upper half of the panel adjust the frequency and amplitude. The controls on the lower half of the panel adjust the timing of the TTL-level trigger signal. This trigger signal (5 μsec duration) is used to externally start the sweep of the multichannel scaler. The phase of the *trigger out* can be set to 0˚ or 90˚ with respect to the *amp out*, or any value in between with the *delay adj* . This makes it is possible to select at which point one wants the MCS sweep to begin with respect to the movement of the Co^{57} source. Simultaneous display of the LVsyn and trigger signals on the scope facilitates this adjustment. For convenience, the rear-panel and front-panel signal connectors are wired in parallel -- using both allows you to monitor the signals on the scope without using extra BNC "T" connectors. Note that the *LVsyn In* signal connector is presently not in use (and is disconnected internally).

The proportional counter signal is first amplified (and buffered) by the preamp before it goes to the amplifier (in NIM Bin). **Note the HV/OPER switch on the preamp -- please make sure that it is in the HV position whenever the high voltage bias is changed (or turned off/on).** The spectroscopy amplifier further amplifies (to a maximum of 10 volts) and shapes (shortens) the signal. Use the scope to observe the signal at each point in this sequence. The signal is typically split after the spectroscopy amplifier. It is routed to the multichannel analyzer (MCA) and the single channel analyzer (SCA). The SCA is used to sort out those pulses corresponding to the 14 keV gamma rays. The SCA window width and baseline voltage must be set appropriately. This can be done with just a scope, but a more elegant solution is to use the MCA in conjunction with the SCA as described below. Manuals for the preamp, amp, SCA, and MCA are available with the *Bench Notes* and should be consulted for operation information.

Multichannel analyzer: The multichannel analyzer (MCA) is used in either one of two modes of operation: pulse height analysis (PHA) or multichannel scaling (MCS). In the PHA mode (as described in the preceding paragraph) it stores a histogram of pulses its input sees versus the voltage of those pulses, which, in this case, is equivalent to the energy of the gamma that produced the pulse. The detector high voltage and spectroscopy amplifier gain together determine the horizontal (energy) scale. The PHA is useful in viewing the total energy spectrum of the radioactive source and selecting the 14 keV line. The SCA output (0.5 μsec long 5 Volt pulses) can be used to enable the PHA in a coincidence mode so that, rather than seeing the entire pulse height spectrum on the PHA, only the pulses corresponding to the 14 keV gammas are recorded. In other words, the PHA will analyze only those input pulses coincident with the logic pulses coming from the SCA. Since the SCA sends out a logic pulse only when a pulse at its input falls within the SCA voltage window, the voltage window settings can be determined

and set by viewing their effect on the PHA spectrum. Once the SCA window has been set, the SCA output pulses can be counted in MCS mode.

MCS mode stores a histogram of pulses its input sees versus time. The MCS consecutively advances through the channels of the selected memory size "dwelling" in each one for a preset amount of time and stores the number of counts received during the dwell time in that particular channel. Thus, by synchronously moving the Co^{57} source and monitoring the counts from the proportional counter in the MCS mode, one obtains a histogram of counts versus velocity (of the Co^{57} source). Furthermore, if the SCA output is used as the input signal to the MCS, then the histogram will represent the number of 14 keV gammas detected versus velocity. Once the velocity scale has been calibrated and converted to Doppler energy shift, then the histogram represents the transmission (and absorption) of 14 keV gammas versus energy.

The pulse height analyzer is a LabVIEW[2] virtual instrument named moss_pha.vi. A multifunction data acquisition card (National Instruments PCI-6070E) interfaces the software with the NIM modules. You can choose either continuous or timed execution. A breakout box (BNC-2110) provides convenient connectors. The following discussion refers to names of BNC connectors on the 2110. In the internal trigger mode, the analyzer processes any signal present at the AI(zero) plug that crosses an adjustable threshold called the lower level discriminator. In external trigger mode, the analyzer waits for a trigger pulse at AI7. The external mode is useful for checking the SCA windows. The PCI-6070E is marginally fast enough to digitize the output pulses from the Ortec 570 amplifier. If you choose a fast shaping time on the amp, you will get strange results from the pha due to undersampling. If desired, the Ortec 542 pulse stretcher can be used to improve the sampling.

The multichannel scaler is named moss_mcs.vi. The multichannel scaler has to sweep synchronously with the Co-57 source modulation. Therefore the only trigger mode offered is “external.” The trigger input is USER2, which in turn is connected to PFI8 (counter0 source) by a hookup wire. The input for event counting is USER1, connected to PFI3 (counter1 source). A typical number of channels is 1000, so the dwell time per channel has to be on the order of tens of microseconds since the Co-57 modulation is on the order of tens of hertz. The onboard clock

[2] A few hints on LabVIEW: Click the ➪ button to run the VI. To stop execution before the timeout expires, use the panel STOP button, not the ● button. Both programs have adjustable “update times.” The display is updated, and data is saved (If the SAVE? Button is switched to YES) once every update time. You will see nothing before the first update time expires. The program only checks the SAVE? Button when it starts; if you switch it to YES while the program is running, nothing will happen.

of the PCI-6070E is used to time the channel advance. A control is provided for the clock speed. Dwell time is the inverse of clock frequency. Set your desired clock frequency before running the program since the clock frequency can't be changed during execution. A hookup wire also connects the clock output (FOUT) to PFI4 (counter1 gate) to define the length of the time bins.

Liquid nitrogen cryostat: In order to measure the Néel transition in iron fluoride, the sample must be cooled a few degrees below the boiling point of nitrogen (77K). To avoid the difficulty and expense of liquid helium, we use pumped nitrogen. The two-liter cryostat mounted behind the Mössbauer apparatus contains the sample on a temperature-controlled copper rod. The iron fluoride is in powder form, mixed with silicone grease to promote temperature uniformity and ease of handling. The cryostat can be rotated 90˚ to place the iron fluoride sample between the source and detector. The sample is located between the beryllium windows, which are nearly transparent to gamma rays. The windows make it possible to keep the sample in vacuum for thermal isolation and measure transmission through it simultaneously. CAUTION: THE BERYLLIUM WINDOWS ARE FRAGILE, POISONOUS, EXPENSIVE AND EASY TO PUNCTURE. DO NOT TOUCH THEM. Once rotated, the cryostat jacket and liquid nitrogen space have to be connected to the vacuum pump. A vacuum manifold with valves and tubing is in the blue cabinet next to the experiment. Ask the faculty or staff for help with this procedure.

A copper cold finger is mounted in the bottom of the liquid container. It meets another smaller copper bar at right angles, which holds the sample. This smaller copper bar is connected to the cold finger through a calibrated copper wire, setting the time constant for cooling at about 25 minutes. A platinum resistance thermometer measures the temperature near the sample. The Lake Shore 330 temperature controller supplies current to a heater (25Ωresistor) in order to reach a setpoint temperature. You can see photographs on the course web site.

A thermocouple gauge measures the pressure in the vacuum jacket. This should always be "low," or less than 10mTorr while the cryostat is cold. A mechanical Bourdon gauge near the top of the cryostat measures pressure in the nitrogen can. Hand-written numbers on the side of the gauge give a rough idea of the temperature in Kelvin. "T" means triple point.

The cool-down procedure is as follows: Contact the staff at least one day before you want to cool down. They will prepare the cryostat by pumping the vacuum jacket overnight. It is best to fill the liquid nitrogen in the morning; the staff can do this as well. Before filling liquid nitrogen, the vacuum jacket must be isolated from the mechanical pump as the pressure in the cold cryostat will be lower than in the pump! If you leave the nitrogen at one atmosphere, the measured temperature of the sample will reach about 83K, well above the Néel temperature. A convenient operating pressure range for work below the Néel temperature is -20 inches Hg to -24 inches Hg. This takes the bath to 70K to 65K – cold enough to see splitting clearly, but still

above the triple point. To reach this pressure, crack the small needle valve open about 1/8 to 1/4 turn. Use the large bellows valve only when you want to go to the lowest possible temperature (about 60K).

The temperature controller is easy to operate. Simply enter a setpoint, and turn on the heater (start with medium power). The controller will determine its PID parameters automatically. For the ambitious, they can be entered manually. As of August 2006, the thermometer has a calibration problem: the measured temperature is nearly 2K greater than the actual temperature.

Michelson interferometer: The velocity of the source has to be calibrated in order to calculate the Doppler shift of the gamma rays. An interferometer measures displacement in units of the wavelength of light, so combined with an accurate measurement of time, you can measure the velocity of the source accurately. The Michelson interferometer has two arms – one ending with a fixed mirror and another ending with a moving mirror, which in this case is next to the Co-57 source. The two beams combine at a photodetector producing interference fringes. Both the reflected beams, as well as the incident beam are split at a 50/50 beamsplitter cube. The cube is not sensitive to polarization. The source of coherent light is a HeNe laser (wavelength 632.8nm). SAFETY WARNING: Follow laser safety procedures at all times. Never look into the laser or at specular reflections. Contain the beampath and all stray reflections above the footprint of the optical table. Use black foamcore to block unwanted beams. The laser is a Class IIIa laser (less than 5mW). Your blink response is enough to protect your eyes in case of accidental exposure. If you prefer to wear laser safety glasses, they can be borrowed from other experiments. Consult the staff.

In order for the beam to reach the moving mirror, remove the lead disk that serves as the sample platform. Follow radiation safety procedures. Three additional mirrors steer the beam up to the source area. Careful alignment is important. The retroreflected beam should retrace the path of the incident beam. Use a white card with a hole in it to check this.

The velocity function is sinusoidal. You can measure its frequency with the HP counter. You can measure v_{max} in two ways. The time required to pass through a few fringes near v_{max} gives v_{max} directly. Otherwise you can count the total number of fringes in a half cycle to get the amplitude of the motion, and then multiply by the frequency. It is best to trigger the scope on the output of the Lvsyn pickup coil.

EXPERIMENTAL PROCEDURE

Setting up the detector: After connecting the apparatus as described in the previous section, the first thing you will need to do is to identify the 14.41 keV line from the Co^{57} source. Set the proportional counter high voltage to +1850 V and look at the output of the amplifier with the oscilloscope. Once you have made all the appropriate adjustments on the amp and scope, you should be able to resolve two prominent energy levels in the midst of the other pulses -- they show up as bright bands. The two levels should be the 14 and the 6 keV lines from the Co^{57} source; the height of the pulse you see is proportional to the energy of the line. You can also see still higher levels clipped by the amplifier. Notice that by placing a thin plastic disk between the source and detector you can cut out one of the lines without drastically altering the other. Now connect the output of the amplifier to the PHA. The horizontal scale corresponds to the height of the pulse and, therefore, to its energy. The main peaks (with the Co^{57} source in a Pd matrix, as it is presently) are the 6 keV line from an Fe x-ray, the 14.41 keV line of interest, a 22 keV Pd x-ray, and a 89 keV Pb x-ray, plus some lines above 100 keV from the Co^{57} decay. You may have to adjust the amplifier gain to see all these peaks. Using the plastic disk or aluminum or copper foils as x-ray filters, you can identify the energy of the displayed lines based on their relative absorption. You can also compare the spectrum with that obtained from an Am^{241} source, which has prominent lines in this energy range. You may wish to perform an "energy calibration" as a double check in identifying the various lines in the pulse height spectrum because, if you end up not using the 14 keV line in your setup there is no hope that the experiment will work. Finally, adjust the gain on the amp until the 14 keV line falls in the upper half of the scale.

Set up the SCA: Now that you have an energy spectrum of the Co^{57} source, learn how to use the SCA to select the detector pulses corresponding to the 14 keV peak in the spectrum. As outlined above, this involves adjusting the voltage window appropriately. The numbers on the dials of the SCA correspond to volts; inspection of the amplifier output on the scope should tell you approximately where to set these dials. Fine adjustments are made by using the SCA output to "gate" the PHA with its coincidence input (PFI0). Remember to select external trigger mode.

Velocity transducer: Begin by setting the frequency of the driver (amplifier) to some nominally low value, like 40 Hz (To monitor the frequency more precisely, use the HP Universal Counter in the *period* mode.). Calibrating the velocity with the Michelson interferometer takes some time, and the lead sample platform has to be disassembled. This can be done either before or after your data runs; you won't want to do it in the middle. The amplitude of the output should be low -- if you *hear* the speaker it is much too high! If you gently touch the speaker cone with

your fingertips, it should feel like a purring pussycat. Typical output of the LVsyn will be in the tens to hundreds of millivolts range, as monitored on the oscilloscope.

MCS setup: Having settled on a transducer frequency, the appropriate dwell time for the MCS must be chosen. This further depends on the number of channels you wish to use. Once started by the external trigger pulse (from the driver control unit), the MCS consecutively advances through the channels of the selected memory size "dwelling" in each one for the preset amount of time and stores the number of counts (pulses from the SCA) received during the dwell time in that particular channel. Having reached the last channel (this is considered as one "sweep" through the channels), the MCS waits for the next trigger pulse and repeats the cycle, adding the new counts to the old. In this way each sweep of the MCS is synchronized to the velocity transducer. However, you must make sure that the product of the dwell time and the number of channels is slightly less than the period of the velocity transducer. It cannot be "exactly" equal to the period and, if it is slightly larger than the period, every other trigger pulse will be missed by the MCS. This would reduce your counting efficiency by a factor of two. The dead time indicator of the mcs program will let you know if you made this mistake. Dead time should be in the range of a few percent.

MEASUREMENTS

The following are suggestions of the kinds of measurements you may wish to undertake. You do not have to do them all and you may wish to duplicate other experiments you find in the literature. Discuss this with your instructor.

Background determination: As is true for any counting experiment, one should always determine how many of the events are due to "background," which we usually consider to be "noise." In the present experiment, a certain number of counts within the selected energy window come from background -- from non-resonant gamma rays that just happen to have energy around 14 keV. You will need to determine how much background there is within your window: the important quantity is the fraction of the counts in the window that come from background. In PHA mode one observes that there is a fairly constant level of background over the full energy range of the spectrum. As an estimate, it is safe to take this as the background level under the peak of interest.

Recoil-free fraction and linewidth: The stainless steel absorber displays the simplest Mössbauer spectrum. Select a fairly thin foil of stainless steel and place it in front of the proportional counter. From the Mössbauer spectrum, measure the depth of the absorption dip. The fractional absorption is defined by $A = (N_\infty - N_{dip})/(N_\infty - N_{bg})$, where N_∞ is the number of counts per channel far from the dip, N_{dip} is the number of counts at the bottom of the dip, and N_{bg} is the number of the N_∞ counts that are due to background. Applying the Debye theory to the properties of the absorber and calculating the expected correction to the absorption will yield the recoil-free fraction of the source. Compare this value of the recoil-free fraction to the theoretical value for the source. How good is the agreement? What does that tell you about the applicability of the Debye theory?

Measure the full width at half maximum (FWHM) from the spectrum. Using the correction formulas from the literature, determine the lifetime of the J=3/2 state. How well does the value compare with the accepted lifetime of $\tau = 1.4 \times 10^{-7}$ sec? Note that the dip does not occur at zero velocity or zero energy shift. Which effects described above are responsible for this?

Isomeric (chemical) shift: Measure the isomeric shift between the Fe^{57} source in Pd and Fe^{57} in various absorbers such as iron, stainless steel, FeF_2, Fe_2O_3, garnet[3] (yttrium iron garnet $Y_3Fe_5O_{12}$ and dysprosium iron garnet $Dy_3Fe_5O_{12}$), $Na_4[Fe(CN)_6]\cdot 10H_2O$, $K_4[Fe(CN)_6]\cdot 3H_2O$, or FeS_2.

Zeeman effect: To observe the Zeeman effect, use an absorber of iron enriched in the isotope Fe^{57} (to make the effect more prominent). Because iron is ferromagnetic, it will probably have a slight magnetization. Obtain a Mössbauer spectrum and determine the locations and depths of the dips (correcting for background). Explain the origin of each dip in terms of the allowed Zeeman transitions. Use the separations between the lines to determine the energy differences Δ_o and Δ_1 between the Zeeman split levels of the J=1/2 and J=3/2 states. Calculate the ratio $|\mu_o/\mu_1|$ of the magnetic moments. Take the magnitudes of the magnetons for the levels to be $|\mu_o| = (0.0903 \pm 0.0007)\mu_N$, $|\mu_1| = (0.1548 \pm 0.0013)\mu_N$[4]. Do your results for $|\mu_o/\mu_1|$ agree? How large is the magnetic field at the location of the iron nucleus? Calculate the relative intensities of the lines. Are they in accord with expectations?

---

[3]Banminger, Cohen, Marinov, and Ofer, "Study of the Internal Fields Acting on Iron Nuclei in Iron Garnets," Phys Rev **122**, 743-748 (1961).

[4] Greenwood and Gibb (1971) p. 102.

Quadrupole splitting: To observe quadrupole splitting you need an absorber containing Fe in a non-symmetric environment. Then the nuclear quadrupole moment interacts with the electric field gradient, splitting the central transition line in two. Use a quadrupole-active absorber, such as sodium nitroprusside, $Na_2[Fe(CN)_5NO]\cdot 2H_2O$, and measure the locations and depths of the dips. Demonstrate theoretically that the dips should be equally spaced about the resonance energy. Are they equally spaced about the zero velocity? If not, explain why. Determine the separation between the dips and evaluate QdE/dz, the product of the quadrupole moment for the J=3/2 state and the field gradient. Given that Q is on the order of 0.1 to 1 barn, how large does this make the field gradient? Is this reasonable?

Temperature shift: Place a sample in a liquid nitrogen bath and measure the Mössbauer spectrum. Observe the shift of the peaks. Is it in the correct direction? How large is it? Is the size of the shift in agreement with the predictions of the second-order Doppler treatment?

The Debye theory makes predictions about the change in fractional absorption with temperature. Because the mean square displacement $\langle x \rangle^2$ depends in a specific way on temperature, one can calculate the change in the recoil-free fraction of the absorber when it is cooled. The recoil-free fraction of the source does not change, so you can predict how much the observed absorption should change. Measure the absorption and compare with expectations.

Antiferromagnetic transition in ferrous fluoride: In this experiment you study the Mössbauer effect in antiferromagnetic FeF_2 which has a transition temperature near the boiling point of liquid nitrogen at 1 atmosphere pressure. A powdered sample is mounted on a cold finger in a cryostat using liquid nitrogen. By pumping on the liquid nitrogen you can lower its temperature to around 60K. The cold finger can be heated and temperature controlled, thus enabling you to probe the order parameter in the vicinity of the transitions and determine the magnetization and the critical exponent, and the Néel temperature. In principle all eight transitions might be observable because the wave functions of the excited state are mixed by the asymmetric electric field gradient tensor.

REFERENCES

General Introduction

A.J. Bearden, P.L. Mattern, and P.S. Nobel, "Mössbauer-Effect Apparatus for an Advanced Undergraduate Teaching Laboratory," Am J Phys **32**, 109-119 (1964).

J.R. Haskins, "Advanced Mössbauer-Effect Experiments," Am J Phys **33**, 646-656 (1965).

H. Lustig, "The Mössbauer Effect," Am J Phys **29**, 1 (1961). Highly recommended as a readable, detailed introduction and a good place to start reading.

G.K. Wertheim, "Resource Letter ME-1 on the Mössbauer Effect," Am J Phys **31**, 1 (1963). AJP Resource Letters are always useful in starting your library research.

Debye-Waller Factor

J. Als-Nielsen, D. McMorrow, *Elements of Modern X-ray Physics*, (J. Wiley, New York, 2000). See page 142.

Selected Reprints

R.L. Mössbauer, "Kernresonanzfluoreszenz von Gammastrahlung in Ir^{191}," Zeitschrift für Physik **151**, 124-143 (1958).

H. Frauenfelder, *The Mössbauer Effect*: *a review - with a collection of reprints*, (W.A. Benjamin, 1962). Cabot QC477.F7

Mössbauer Effect: Selected Reprints, published by AIP for the AAPT (1963). Cabot QC491.A44

Antiferromagnetic transition in FeF_2

G.K. Wertheim and D.N.E. Buchanan, *Temperature Dependence of the Fe hfs in FeF_2 below the Néel temperature,* Phys. Rev 161, 478 (1967).

Monographs

J. Danon, *Lectures on the Mössbauer Effect*, (Gordon & Greach, NY, 1968). Cabot QC490.L4

D.P.E. Dickson and F.J. Berry (editors), *Mössbauer Spectroscopy*, (Cambridge Univ Press, 1986). Cabot QC491.M6135

T.C. Gibb, *Principles of Mössbauer Spectroscopy*, (Chapman & Hall, London, 1976). Useful introduction followed by in-depth treatment of chemical effects. Cabot QC491.G52

N.N. Greenwood and T.C. Gibb, *Mössbauer Spectroscopy*, (Chapman & Hall, London, 1971). Cabot QC490.G74

U. Gonser (editor), *Mössbauer Spectroscopy*, (Springer-Verlag Topics in Applied Phys - Vol 5, NY, 1975). The first chapter by Gonser is a good introduction. Phys Res QC491.M912

G.K. Wertheim, *Mössbauer Effect: Principles and Applications*, (Academic Press, NY, 1964). Cabot QC490.W4

The Exotic Side of the Mössbauer Effect

Once the extension of experimental work to lines as narrow as those of Fe^{57} was achieved, it became possible to observe the gravitational red shift within an earth-bound laboratory. Robert Pound and Glen Rebka performed their historic experiments here at Harvard in the Jefferson Physical Laboratory. They were able to demonstrate that the frequency of gamma radiation measured at its source (on the building's roof) differed from the frequency measured in the basement. The incredibly small shift (about 1 part in a million billion) showed that clocks run slower in the basement than the roof because, being closer to the Earth, the gravitational field, and hence the space-time curvature, is larger there. The faster clock on the roof would read a lower frequency of gamma radiation and thus the wavelength would be longer, or red-shifted. The red-shift experiment was initially proposed in the first paper (below) and conclusive results were given in the second. Later it was demonstrated that temperature effects (see page B-2-8 of this write-up) could have completely obscured the gravitational shift. The third paper presents the first conclusive experiments taking temperature effects into account

R.V. Pound and G.A. Rebka, Jr., "Gravitational Red Shift in Nuclear Resonance," Phys Rev Letters **3**, 439 (1959).

R.V. Pound and G.A. Rebka, Jr., "Apparent Weight of Photons," Phys Rev Letters **4**, 337 (1960).

R.V. Pound and G.A. Rebka, Jr., "Variation with Temperature of the Energy of Recoil-Free Gamma Rays from Solids," Phys Rev Letters **4**, 274 (1960).